Identigram/Watermark Removal using Cross-channel Correlation

Jaesik Park Yu-Wing Tai In So Kweon
Korea Advanced Institute of Science and Technology (KAIST)
jspark@rcv.kaist.ac.kr, yuwing@kaist.ac.kr, iskweon@kaist.ac.kr

Abstract

We introduce a method to repair an image which has been stamped by an identigram or a watermark. Our method is based on the cross-channel correlation which assures the co-occurrence of image discontinuities and correlation of color distributions across different color channels of an image. Using blind source separation, we find the transformation of color space which separates the structures of identigram and that of the original image into two different individual color channels. To repair the image contents in the corrupted channel, we formulate the problem using Bayes' rule where the prior and the likelihood probabilities are defined based on the cross-channel correlation assumption. We compare our results with results from inpainting and texture synthesis-based hole filling techniques. Our results are pleasable for real-world examples and have the maximum PSNR for synthetic examples.

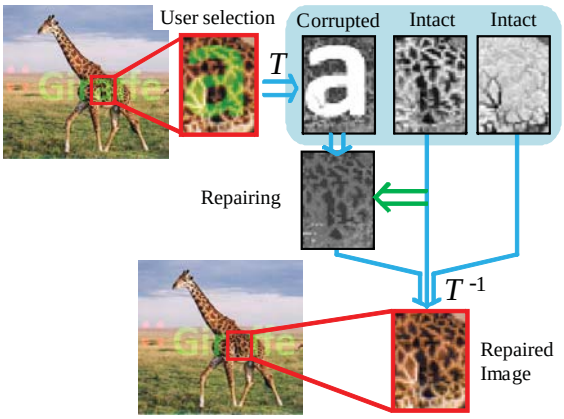

Figure 1. An overview of our framework. For the user selected region, we compute a transformation that minimizes the correlation of image structures across different color channels. Using the cross-channel correlation, we repair the image content in the corrupted channel based on the image structures from the intact channel. Finally, we reverse the transformation to produce the repaired image in the original color space.

1. Introduction

Identigram (a compound word of identity and hologram) is a watermark added on top of an image for protecting the copyright and the identification of an image. These watermarks are security patterns which partially occlude the image contents such that other people cannot edit or process the protected image easily while the original image can still be recognized by a person. A typical example of identigram is the hologram printed on top of the identity photo in the U.S. passport or in the identity card. In this paper, we describe a method to remove the identigram/watermark digitally from a single RGB color image.

Our method is based on the observation that these identigrams/watermarks only partially occlude an image where the original image structures still exists even in the corrupted image regions. Since there is usually no correlation between the identigram/watermark and the protected image, we assume that there is a transformed color space in which the structures of the identigram/watermark and that of the protected image can be well separated. We use the blind source separation technique [13] to find the transformation of color space which minimizes the mutual information of image structures across different color channels. We called the transformed color channel that contains structures of identigram/watermark "corrupted channel", and the transformed color channel that contains structures of the original image "intact channel'. Our goal is then to repair the image contents in the corrupted channel with the guidance of image structures from the intact channel. Our final result is a repaired image in the original color space which the identigram/watermark has been successfully removed. Since identigram is usually another physical layer printing on top of the original image, we assume the watermarks are additive. Figure 1 shows the overview of our method.

To repair the image contents in the corrupted channel, we use the cross-channel correlation. The usage of cross-channel correlation is based on the statistical relationship between different color channels of an image, such as the co-occurrence of image edges, texture patterns, shadings and homogeneous color regions. From the image structures

in the intact channel, our method infers the image structures in the corrupted region and use the structures to guide the repairing process. This is done by using a constrained hole filling algorithm formulated by using Bayes' rule. Our experimental results show that our method can adaptively repair the corrupted regions with the original image structures inferred from the intact channel.

2. Related Works

There are various approaches for watermark attacking and watermark removal [17, 15, 11, 16, 18]. Early works in watermark attacking [17, 15] aim to remove the recognition ability of the hidden watermark pattern. Their goal is not to recover the original image, but to make the hidden watermark pattern useless in identifying the original source of an image. In [16], van Leest *et al.* proposed a reversible watermarking algorithm which allows the original image to be recovered from a watermarked image. But their algorithm requires careful design of watermarking pattern and knowledge of watermark process. Work in [11] removes visible watermark in JPEG compressed image by exploiting self-similarities within an image. Nevertheless, their goal is still on watermark attacking instead of image recovery. Recent work in [18] analyzes the DCT coefficient of a watermarked image to detect the watermarked regions and then recover the original image content. However, their algorithm still requires knowledge of watermark process. For a scanned identity photo, the identigram is physically printed on top of the digital photo. Hence, such method that requires knowledge of watermark process might not be applicable.

Image inpainting/completion techniques [2, 1, 4, 8, 14, 9, 6] can also be used for repairing the regions corrupted by identigram/watermark. The image inpainting algorithm proposed by Bertalmio *et al.* [2] is based on PDE diffusion equations which propagates surrounding structures and intensities to the corrupted regions. Image inpainting techniques work well for repairing small gaps and thin structures. However, for larger missing regions, the repaired regions may be blurry. Example-based approaches [1, 4, 8, 14] fill in the missing regions using texture synthesis [5]. In order to better preserve image structures and to allow better user controls, Sun *et al.* [14] proposed an algorithm which propagates image structures according user scribbles to guide the hole filling process. Mairal *et al.* [9] proposed an image restoration algorithm which uses sparse representation of image patch with dictionary learning for simultaneously image denoising and reconstruction. Hays and Efros [6] use internet images for hole filling which demonstrates high quality repairing results even for holes with very large missing areas. These image inpainting/completion techniques have been proven to produce high quality results in repairing holes inside an image. However, these techniques tend to fill in missing areas with new contents which does not respect to the partial image information remained in the identigram/watermark regions.

Our method can be classified as image completion technique. Unique in our method is the structure separation algorithm which separates the structures of identigram/watermark and the structures of the original image into two different channels before repairing. In the hole filling process, we take the structures in the intact channel into account. Hence, we can achieve results with higher quality comparing to the results from previous works. However, since our algorithm is designed for repairing regions that are only partially corrupted, our algorithm is not suitable for general cases where the whole repairing regions are missing.

3. Algorithm

In this section, we describe our identigram/watermark removal algorithm. Figure 1 shows the overview of our algorithm. We first describe our blind source separation algorithm for structure separation. Then, we describe our hole filling algorithm for repairing the image structures in the corrupted channel.

3.1. Structure separation via color space transformation

Our algorithm starts with user inputs which identify the regions that are contaminated by the identigram/watermark. From the user selected regions, we find a transformation of color space such that the correlation of image structures across different channels are minimized. This is based on the assumption that there is no relationship between the structures of identigram/watermark and that of the original image. We adopt the blind source separation technique [13] to serve our purpose:

$$I'(x) = T[I(x)], \tag{1}$$

where I and I' are the image in the original color space and the image in the transformed color space respectively, and T is a non-singular matrix which describes the transformation of color space from I to I'. Figure 2 shows an example which separates the structures of paints and wood textures into the corrupted channel and the intact channel respectively.

We evaluate the transformation matrix T by measuring the mutual information across different color channels after transformation. We define the mutual information of two color channels, C_1 and C_2, by using the Kullback-Leibler (KL) [3, 12] distance between image histograms:

$$\mathcal{M}(C_1, C_2) = \sum_{l_{C_1}, l_{C_2} \in \mathcal{L}} H(l_{C_1}, l_{C_2}) \log \frac{H(l_{C_1}, l_{C_2})}{H(l_{C_1}) H(l_{C_2})}, \tag{2}$$

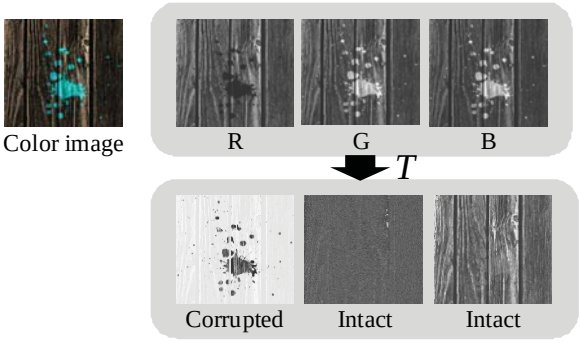

Figure 2. An example of structure separation using color channel transformation. In this example, the corrupted regions contaminate the three color channels in the RGB color space. Our method finds a transformation of color space such that the corrupted regions and the original structures are separated into two different channels.

where $H(l_{C_1})$ and $H(l_{C_2})$ are the probabilities for certain intensity levels l_{C_1} and l_{C_2} appear in C_1 and C_2, respectively, $H(l_{C_1}, l_{C_2})$ is the joint probability for l_{C_1} and l_{C_2}, and $\mathcal{L}$ is a set of all possible intensity levels in image histograms. In order to reduce the dependency on the brightness of two channels, $\mathcal{M}(C_1, C_2)$ in Equation (2) is normalized by dividing it by the mean self-information of C_1 and C_2:

$$\frac{1}{2}[-\sum_{l_{C_1}\in\mathcal{L}} H(l_{C_1})\log H(l_{C_1}) - \sum_{l_{C_2}\in\mathcal{L}} H(l_{C_2})\log H(l_{C_2})]. \quad (3)$$

In order to find the transformation of color space efficiently, we follow the previous work in [13] which decomposes T into a rotation matrix R and a pre-whitening matrix V:

$$T = R(\phi)V, \quad (4)$$

where ϕ is the rotation angle of R. The pre-whitening is a common preprocessing step in independent component analysis [7] which de-correlates the color samples in the original color space by transforming the covariance matrix of color samples into an identity matrix. The pre-whitening matrix V can be computed effectively using eigen-value decomposition. Now, we reduce the search space of the transformation matrix T by only searching the optimal rotation matrix R that minimizes the mutual information across different color channels. In our implementation, we evaluate the rotation matrix for each 5° between -90° to 90°.

In practice, we have three color channels, our method finds the transformation of color space such that the mutual information of any two transformed color channels is minimized. After the color space transformation, we ask users to select the channel that contain the identigram/watermark as the corrupted channel, and the channel that contain the original image structures as the intact channel. From the corrupted channel, we detect the corrupted regions by computing the correlation of pixel intensity between the corrupted channel and the intact channel. After thresholding, we obtain a mask for the corrupted regions in the corrupted channel.

3.2. Constrained Hole Filling for Corrupted Region Repairing

In this section, we describe our method for repairing the corrupted regions in the corrupted channel using constrained hole filling. We first consider the case where there are only two channels, the corrupted channel and the intact channel, in the transformed color space and describe our method based on the two channel inputs. Then, we will describe an extension of our method for the cases when there are more than one corrupted channel in the transformed color space or when the transformed color space still contains mixed structures across different channels.

Let $\mathcal{C}$ and $\mathcal{I}$ be the image in the corrupted channel and the image in the intact channel respectively, Ω be the corrupted region, and $\partial\Omega$ be the boundary of the corrupted region. We formulate our problem using Bayes' rule as follows:

$$\begin{aligned} \mathcal{C}_\Omega^* &= \arg\max_{\mathcal{C}_\Omega} P(\mathcal{C}_\Omega|\mathcal{I}_\Omega, \mathcal{C}_{\partial\Omega}) \\ &= \arg\max_{\mathcal{C}_\Omega} P(\mathcal{I}_\Omega|\mathcal{C}_\Omega)P(\mathcal{C}_{\partial\Omega}|\mathcal{C}_\Omega)P(\mathcal{C}_\Omega), \quad (5) \end{aligned}$$

where $\mathcal{C}_\Omega^*$ is the repaired image in $\mathcal{C}$, $P(\mathcal{I}_\Omega|\mathcal{C}_\Omega)$ is the likelihood probability of $\mathcal{C}_\Omega$ having similar structures as $\mathcal{I}_\Omega$ in Ω, $P(\mathcal{C}_{\partial\Omega}|\mathcal{C}_\Omega)$ is the likelihood probability corresponding to the boundary constraint of $\mathcal{C}_\Omega$, and $P(\mathcal{C}_\Omega)$ is the prior probability of $\mathcal{C}_\Omega$.

We define $P(\mathcal{I}_\Omega|\mathcal{C}_\Omega)$ as the pairwise similarity between pixels in $\mathcal{C}_\Omega$ and $\mathcal{I}_\Omega$:

$$P(\mathcal{I}_\Omega|\mathcal{C}_\Omega) = \prod_{x\in\Omega}\prod_{y\in N(x)} \exp(-\phi(x, y, \mathcal{C}_\Omega, \mathcal{I}_\Omega)), \quad (6)$$

where x and y are pixel coordinates, $N(x)$ is the first order neighborhood of x,

$$\phi(x, y, \mathcal{C}_\Omega, \mathcal{I}_\Omega) = w_{x,y}(\mathcal{C}_\Omega(x) - \mathcal{C}_\Omega(y))^2, \quad (7)$$

$$w_{x,y} = \frac{1}{S}\exp\left\{-\frac{(\mathcal{I}_\Omega(x) - \mathcal{I}_\Omega(y))^2}{\sigma_\mathcal{I}^2}\right\}, \quad (8)$$

$\sigma_\mathcal{I}$ is the standard deviation that controls the similarity weight between $\mathcal{C}_\Omega(x)$ and $\mathcal{C}_\Omega(y)$, and S is a normalization factor.

Equation (6) defines a weighted similarity between $\mathcal{C}_\Omega(x)$ and $\mathcal{C}_\Omega(y)$ using the pixel similarity between $\mathcal{I}_\Omega(x)$ and $\mathcal{I}_\Omega(y)$. If the intensity between $\mathcal{I}_\Omega(x)$ and $\mathcal{I}_\Omega(y)$ is similar, we give a large similarity weight for $\mathcal{C}_\Omega(x)$ and $\mathcal{C}_\Omega(y)$. In contrast, if $\mathcal{I}_\Omega(x)$ and $\mathcal{I}_\Omega(y)$ are very different which is potentially to be an image edge, we allow $\mathcal{C}_\Omega(x)$ and $\mathcal{C}_\Omega(y)$

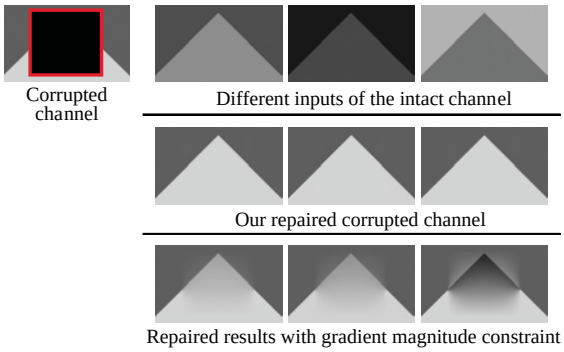

Figure 3. A synthetic example to demonstrate the effect of our structural constraint. The first row shows the corrupted image (corrupted area is indicated by the red box) and the images in the intact channel with different intensity values. The second row shows our repaired images by applying the structural constraint from the intact channel. The discontinuities in the repaired regions are well aligned the discontinuities in the intact channel. For reference, we show the results on the third row which we enforce the gradient magnitudes of the repaired images to be the same as the gradient magnitudes in intact channels.

(a) (b) (c)

Figure 4. The effects of color distribution prior. (a) Input image, the transformed color space is shown in Figure 2. (b) Repaired result without the color distribution prior. (c) Repaired result with color distribution prior. Note that the textures within the corrupted regions are well repaired.

having different intensity values. This weighted similarity measurement allows the repaired image structures in $\mathcal{C}_\Omega^*$ to be aligned with the image structures in $\mathcal{I}_\Omega$. Note that Equation (6) only enforces the alignment of images structures between $\mathcal{C}_\Omega^*$ and $\mathcal{I}_\Omega$, but the gradient magnitudes in $\mathcal{C}_\Omega^*$ and $\mathcal{I}_\Omega$ can be different. Figure 3 shows the effects of Equation (6).

We define $P(\mathcal{C}_{\partial\Omega}|\mathcal{C}_\Omega)$ as:

$$P(\mathcal{C}_{\partial\Omega}|\mathcal{C}_\Omega) = \prod_{x\in\partial\Omega} \exp(-\frac{(\mathcal{C}_{\partial\Omega}(x) - \mathcal{C}_\Omega(x))^2}{\sigma_\mathcal{C}^2}), \quad (9)$$

where $\sigma_\mathcal{C}$ is the standard deviation that controls the weights of the boundary constraint which favors the boundary of $\mathcal{C}_\Omega^*$ having similar intensity with $\mathcal{C}_{\partial\Omega}$ for seamless connection between the repaired and the untouched original image regions.

We define $P(\mathcal{C}_\Omega)$ by assuming that the color distribution of repaired regions follows the color distribution of nearby uncorrupted regions. From the user selected areas, we model the color distribution of uncorrupted area in the transformed color space using the Gaussian mixture model (GMM). For each pixel within the corrupted regions, we choose the Gaussian distribution that has minimal distance to the value of the pixel in the intact channel. We model $P(\mathcal{C}_\Omega)$ as:

$$P(\mathcal{C}_\Omega) = \prod_{x\in\Omega\setminus\partial\Omega} \exp(-\frac{(\mathcal{C}_\Omega(x) - \mu_g)^2}{\sigma_g^2}), \quad (10)$$

where μ_g and σ_g are the mean and the standard derivation of the chosen Gaussian distribution in the corrupted channel. Figure 4 shows the effects of this prior term.

Combining Equation (5), (6), (9) and (10) and taking the negative log operation, we obtain a set of linear equations:

$$\begin{aligned} \mathcal{C}_\Omega^* \quad = \quad & \arg\min_{\mathcal{C}_\Omega} \sum_{x\in\Omega} \sum_{y\in N(x)} w_{x,y}(\mathcal{C}_\Omega(x) - \mathcal{C}_\Omega(y))^2 + \\ & \lambda_1 \sum_{x\in\partial\Omega} (\mathcal{C}_{\partial\Omega}(x) - \mathcal{C}_\Omega(x))^2 + \\ & \lambda_2 \sum_{x\in\Omega\setminus\partial\Omega} (\mathcal{C}_{\partial\Omega}(x) - \mu_g)^2 \end{aligned} \quad (11)$$

where $\lambda_1 = 1/\sigma_\mathcal{C}^2$ and $\lambda_2 = 1/\sigma_g^2$ are the relative weight between the energy terms. We set $\sigma_\mathcal{I}^2 = 5^{-4}$ and $\sigma_\mathcal{C}^2 = 10^{-6}$ for $\mathcal{C}, \mathcal{I} \in [0, 1]$ and σ_g^2 is estimated from the color distribution in the uncorrupted regions. Equation (11) can be solved effectively using standard LU factorization based sparse linear solver.

The repairing method in Equation (11) assumes that there are only two channels and the separation of structures in the corrupted channel and the intact channel is perfect. In practice, we have three color channels. We observe that the third channel (Neither corrupted channel nor intact channel) in the transformed color space usually contains mixed structures of the corrupted channel and the intact channel as shown in Figure 5. Although we can consider this mixed channel as a corrupted channel and repair the mixed channel using the method in Equation (11), this method sometimes discards the original structures that are remained in the mixed channel.

In order to remove the identigram/watermark in the mixed channel while protecting the remaining original image structures, we use an iterative method. We consider the structures of identigram/watermark in the mixed channel as residual errors. After we repair the corrupted channel in the first iteration, we reverse the transformation and apply the whole algorithm again to find another transformation coordinates for repairing. Since the dominant structures from the identigram/watermark has been repaired in the first iteration, the estimated transformation in the second iteration separates the residual errors into the corrupted channel.

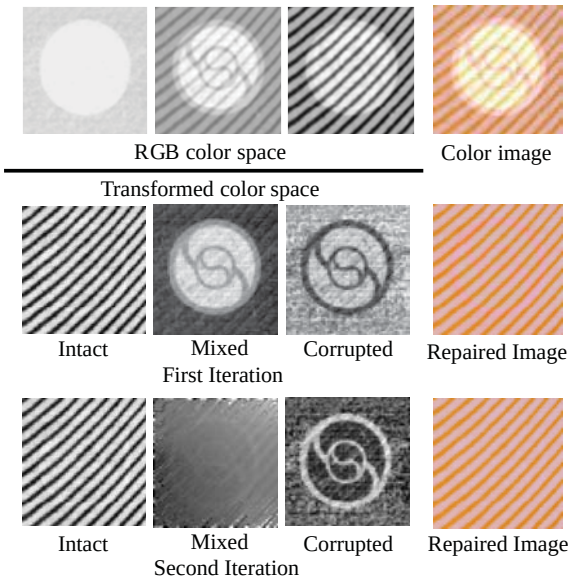

Figure 5. Iterative repairing of our algorithm. First row: input color image and its corresponding images in RGB channels. Second row: the transformed color space for the first iteration and our repaired result. Third row: the transformed color space for the second iteration and our repaired result. Note that the residual errors in the mixed channel in the first iteration is well separated in the transformed color space in the second iteration.

	Apple	Texture	Street
Inpainting [2]	15.76	11.75	15.37
Poisson [10]	16.71	13.13	15.55
Exemplar [4]	12.42	15.57	12.75
Sparse [9]	14.34	14.09	15.86
Ours	**18.46**	**18.18**	**17.72**

Table 1. Quantitative comparison on the Apple(Figure 6), the Texture(Figure 7), the Street dataset(Figure 8). The error is measured in PSNR for the corrupted region. Our algorithm shows the best PSNR among the compared algorithms.

Hence, we can repair the residual errors in the new color space in the second iteration without destroying the structures of the original image in the mixed channels in the first iteration. The iteration of our algorithm can continue until no more corrupted regions are detected in the corrupted channel. In our experiments, we find that two iterations is sufficient to produce high quality repairing results. Figure 5 shows an example using this iterative scheme for repairing.

4. Experimental Result

4.1. Synthetic examples

We first compare our results with results from previous works on synthetic examples in Figure 6, 7 and 8. The synthetic examples were created by using the "hard light" blending mode from Photoshop ^{TM} CS5. Figure 6 is an example which contains sharp image edges; Figure 7 is a texture images with many repeated textures which is suitable for example-based hole filling algorithm; Figure 8 is a natural image with complicated structures and textures. Our results are compared with poisson image editing [10], image inpainting [2], exemplar-based texture synthesis [4], and image restoration using sparse representation [9]. Since these methods repair the corrupted regions without considering the partial image structures in the corrupted region, their hole filling results contain synthesized new image content which does not align with the original image structures. On the other hand, our method produces natural results which does not show any obvious artifacts in the repaired regions. Quantitative comparisons in terms of PSNR are presented in Table 1.

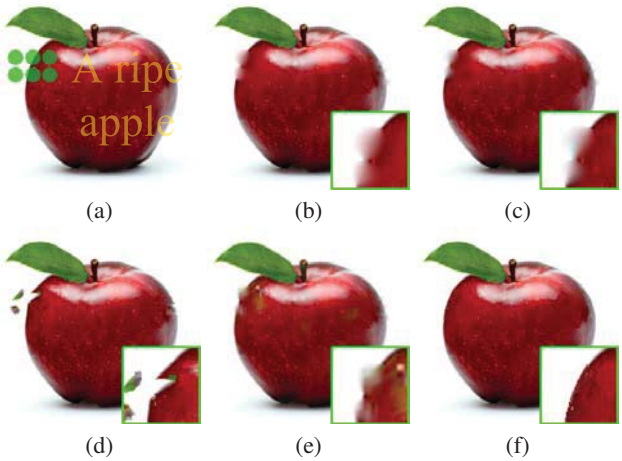

Figure 6. (a) A semi-transparent watermark is overlaid on an apple image. Results obtained by (b) Poisson Image Editing [10] with zero gradient assigned to the hole filling regions, (c) image inpainting [2], (d) exemplar based inpainting [4] (e) sparse representation [9] and (f) our proposed method.

4.2. Real-World Examples

Figure 9 and Figure 10 show real-world examples for identigram removal where input images are severely distracted by security patterns. These example images can be found from google image search engine with keyword "identigram"[1]. We show the transformed color space and our repaired results in Figure 9 and Figure 10. We compare our result with results from image inpainting [2] and exemplar-based texture synthesis [4] in Figure 9. Since the corrupted regions are relatively large and are highly structured, the results from previous works cannot repair the corrupted region properly. On the other hand, our approach extracts the original image structures through color space transformation which allows the partial information of the original image to be used to repair the corrupted regions in the corrupted channel. Note that our results do not syn-

[1] $http://www.bundesdruckerei.de/$

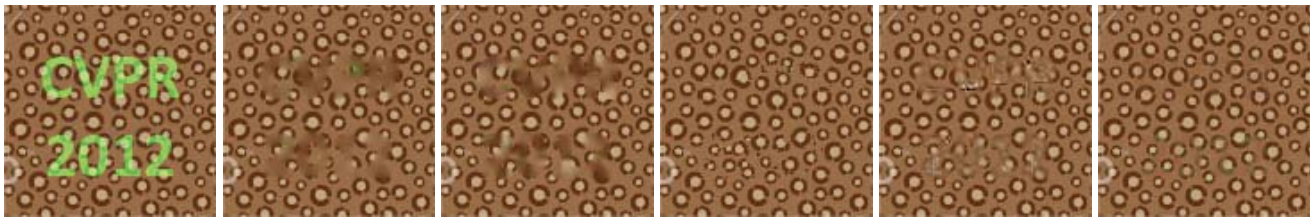

(a) (b) (c) (d) (e) (f)

Figure 7. (a) A text is overlaid on the dot pattern. Results obtained by (b) Poisson Image Editing [10] with zero gradient assignment, (c) image inpainting [2], (d) exemplar based inpainting [4], (e) sparse representation [9] and (f) our proposed method.

(a) (b) (c)

(d) (e) (f)

Figure 8. (a) A corrupted image. This image shows more complicated structures. Results obtained by (b) Poisson Image Editing [10] with zero gradient assignment, (c) image inpainting [2], (d) exemplar based inpainting [4], (e) sparse representation [9] and (f) our proposed method.

thesize any new image contents comparing to results from previous works. Although our results are not perfect, our approach enhances the original images to allow users better reveal the contents covered by the identigram/watermark.

Our approach is not limited to identigram/watermarked removal. We tested our algorithm to other problems. Figure 11 shows an example of highlight removal and Figure 12 shows an example of dust removal. Our method is able to remove the highlighted yellow regions while protecting the original text in Figure 11. Comparing our result with result in [19], our result may not be physically correct, but our result is natural.

5. Discussion and Limitations

Our algorithm is designed to remove identigrams that are physically printed on top of identity photos. When applying our algorithm to general watermark removal, our algorithm might fail when the watermarks were added digitally through multiplications or other methods which the additive color model of identigram is violated. In such cases, linear transformation of color space might not be able to separate the structures of identigram/watermark from the structures of the original image. We regard this problem as a fundamental limitation to the assumption of our approach.

We note that in our results in Figure 9 and Figure 10, when input images are highly compressed, our repaired results still contains some identigram/watermark patterns. This is because compression mixes the structures of identigram/watermark with the structures of the original image. Hence, blind source separation cannot perfectly separate the structures into two individual channels even with the iterative method. We have also noted that when the watermarks

(a) (b) (c) (d)

(e) (f) (g)

Figure 9. A real-world example for identigram removal. (a) A scanned identify card image with security pattern. (b)(c)(d) The transformed color coordinate for repairing. Repaired images using technique from (e) image inpainting [2], (f) image repairing [8], and (g) our method.

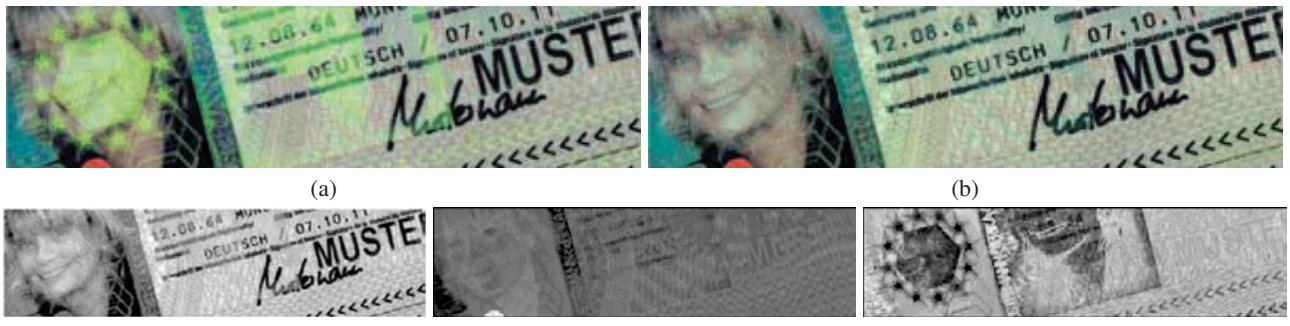

(a) (b)

(c) (d) (e)

Figure 10. Another real-world example for identigram removal. (a) Input image. The facial part of the image is severely distracted. (b) Our result. The image becomes clear and the women is now recognizable. (c)(d)(e) The transformed color coordinate for repairing.

are colorful, or when the watermarks overlaid on colorful regions, a global transformation of color space is not the best solution. Indeed, our approach performs better when a user select a small region to process instead of processing the image as a whole. Such local processing allows each local regions to have different transformed color space and hence performs better in colorful regions.

In situation when there are remaining identigram structures in the intact channel, we can apply our algorithm iteratively. The iterative refinement alleviates these errors by using different color space transformation in each iteration. Nevertheless, if the remaining identigram structures are significant, our approach will be failed since those structures will be regarded as the structures from the original image.

Finally, our constrained hole filling algorithm is developed based on the cross-channel correlation assumption. This assumption is valid for most natural images, but there can be a case that there is no correlation across different channels after the color space transformation. This happens when the structures of the original image span less than

(a) (b)

Figure 11. Highlight removal. (a) Input image. (b) Our result.

(a) (b) (c)

Figure 12. Dust removal. (a) Input image. (b) Our result. (c) Result from Zhou *et al*. [19]

three dimensions, and when the identigram lies on the null space of the original image structures. But statistically, this situation is rare.

6. Conclusion

In this paper, we have presented a method to remove identigram/watermark from a single multi-channel image. Our approach is based on the cross-channel correlation assumption. We apply the blind source separation across different color channels to separate the structures of identigram/watermark and the structures of original image into the corrupted channel and the intact channel respectively. A constrained hole filling algorithm is proposed to repair the corrupted regions in the corrupted channel with an assistance of image structures from the intact channel. We demonstrate our algorithm on various examples. Our results are better than the results from inpainting and texture synthesis-based algorithms. In our current implementation, we identify the corrupted channel and the intact channel manually after the blind source separation. In the future, we shall study how to identify the corrupted channel and the intact channel automatically. We shall also study how to extend our method to non-linear transformation of color space to tackle some of our current limitations.

7. Acknowledgements

We thank the anonymous reviewers for their valuable comments. This research is supported in part by the MKE, Korea, under the Human Resources Development Program for Convergence Robot Specialists support program supervised by the NIPA and the National Research Foundation of Korea (No.2011-0018250). Yu-Wing Tai is supported by the MCST and KOCCA in the Culture Technology(CT) Research & Development Program 2011 and the National Research Foundation of Korea (No. 2011-0013349).

References

[1] A. Barret and A. Cheney. Object-based image editing. *ACM Trans. Graph.*, 21:777–784, 2002.

[2] M. Bertalmio, G. Sapiro, V. Caselles, and C. Ballester. Image inpainting. In *SIGGRAPH*, pages 417–424, 2000.

[3] T. M. Cover and J. A. Thomas. Elements of information theory. *Wiley, New York*, 1991.

[4] A. Criminisi, P. Pérez, and K. Toyama. Object removal by exemplar-based inpainting. In *CVPR*, 2003.

[5] A. Efros and T. Leung. Texture synthesis by non-parametric sampling. In *CVPR*, pages 1033–1038, 1999.

[6] J. Hays and A. A. Efros. Scene completion using millions of photographs. *ACM Trans. Graph.*, 26, 2007.

[7] A. Hyvarinen and E. Oja. Independent component analysis: Algorithms and application. *Neural Networks*, pages 411–430, 2000.

[8] J. Jia and C.-K. Tang. Image repairing: Robust image synthesis by adaptive nd tensor voting. In *CVPR*, 2003.

[9] J. Mairal, M. Elad, and G. Sapiro. Sparse representation for color image restoration. *IEEE Trans. on Image Processing*, pages 53–69, 2007.

[10] P. Pérez, M. Gangnet, and A. Blake. Poisson image editing. *ACM Trans. Graph.*, 22:313–318, July 2003.

[11] C. Rey, G. Doerr, G. Csurka, and J.-L. Dugelay. Toward generic image dewatermarking? In *ICIP*, volume 2, pages 633–636, 2002.

[12] Y. Schechner, N. Kiryati, and J. Shamir. Blind recovery of transparent and semireflected scenes. In *CVPR*, 2000.

[13] H. Stogbauer, A. Kraskov, S. A. Astakhov, and P. Grassberger. Least dependent component analysis based on mutual information. *Phys. Rev.*, 2004.

[14] J. Sun, L. Yuan, J. Jia, and H.-Y. Shum. Image completion with structure propagation. *ACM Trans. Graph.*, 24, 2005.

[15] K. Tsang and O. Au. A review on attacks, problems and weaknesses of digital watermarking and the pixel reallocation attack. In *SPIE Security and Watermarking of Multimedia Content III*, volume 4314, pages 385–393, 2001.

[16] A. van Leest, M. van der Veen, and F. Bruekers. Reversible image watermarking. In *ICIP*, 2003.

[17] S. Voloshynovskiy, S. Pereira, T. Pun, J. Eggers, and J. Su. Attacks on digital watermarks: classification, estimation based attacks, and benchmarks. *IEEE Communications Magazine*, 39(3):118–126, 2001.

[18] A. Westfeld. A regression based restoration technique for automated watermark removal. In *ACM workshop on Multimedia and security*, 2008.

[19] C. Zhou and S. Lin. Removal of image artifacts due to sensor dust. In *CVPR*, 2007.